NIR extinction coefficients in Paranal

E. Mason[1], G. Lombardi[2], C. Lidman[1] and A. O. Jaunsen[3]

[1] ESO, Chile emason@eso.org, clidman@eso.org
[2] University of Bologna, Italy gianluca.lombardi@oabo.inaf.it
[3] Institute of Theoretical Astrophysics, Norway a.o.jaunsen@astro.uio.no

1 Introduction

The atmosphere is opaque and attenuates the starlight. The actual attenuation (i.e. extinction in mag/airmass) depends on the waveband of the observations and the astronomical site. It is possible to measure the atmospheric extinction of a site by fitting the Bouguer curve.

ISAAC at UT1 is a NIR imager and spectrograph which is in operation since 1999. Its calibration plan foresees the observation of a photometric standard star during the evening twilight whenever the instrument is in use. The ESO archive (http://archive.eso.org) contains a large amount of photometric standard stars which can be used to characterize the NIR extinction of the Paranal site. This has been done by us. Here we presents our results, together with the color term corrections applicable to the ISAAC SW filters.

2 Determining the extinction

2.1 The sample

We retrieved from the ESO archive all the Persson standard stars (Persson et al. 1998) which have been observed with ISAAC SW arm in the broad band filters JJsH and Ks during photometric or clear nights. This resulted in data from 494 different nights between Jan 2000 and Jun 2004, 40 different stars and 578 data points in the J band, 606 in Js, 607 in H and 678 in Ks. We restricted ourselves to the Persson standards[4] due to the similarity of the ISAAC filter transmission curves and that at Las Campanas Observatory (LCO). This reduces the color terms to a correction of the second order.

The data were all reduced with the eclipse pipeline (ISAAC v 5.0.0). Each data point ($ZP(i)$) resulted from the eclipse recipe *zpoint* after having removed the ghost and dark, flat-fielded and corrected for non linearity each frames (see ISAAC Pipeline User Manual for more details). Figure 1 plots the computed $ZP(i)$. The figure shows that the points distribution can be divided in subsample or periods, each delimited by a mirror re-coating and/or an instrument intervention. We analyzed (Sec. 2.2) each period separately.

[4]The calibration plan of ISAAC occasionally uses also UKIRT standard stars.

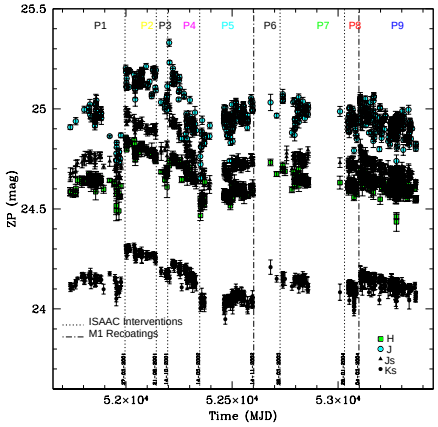

Fig. 1. The JJsH and Ks zero points as computed by the eclipse pipeline. They are not corrected for extinction. Note that each subsample/period is identified by the label P_i, with i integer between 1 and 9.

2.2 Analysis of the sample

We started by removing any obvious trend of the data points within each period. The ZPs are expected to change after an instrument intervention as it may affect the instrument configuration. They also decrease in time due to the progressively reduced reflectivity of the mirror (because of dust and/or oxidation of the mirror coating). Therefore, we applied a linear fit to the $ZP(i)$ vs time, t, and removed the time trend by adding the amount $ZP(t = 0) - ZP(t_i)$ to each zero point $ZP(i)$. Note that we identified a total of 9 periods, but we applied the above correction to just 5 of them. The remaining 4 periods either do not show a clear decrease of the ZP versus time or contain too few data points.

We continued by checking for possible dependency of the computed ZP on the precipitable water vapor (PWV) content in the atmosphere. Indeed, the NIR atmospheric extinction is sensitive to the H_2O column abundance above the site (Manduca & Bell 1979). Figure 2 (left panel) shows that there is a seasonal variation of the PWV in Paranal; the amount of measured PWV being larger during the so called Bolivian winter (i.e. the trimester Jan-Mar). Figure 2 (right panel) also shows how the ZPs decrease for larger PWV values. We computed the median PWV value of 2.279 mm for the period 2000-2004 and rescaled all the ZP(i) (already corrected for time dependence) to such median value.

Finally we plot the "cleaned" $ZP(i)$ versus airmass and fit the Bouguer curve to each period and each filter (Figure 3). The extinction coefficient (i.e. the slope of the linear fit) for each period are reported in Table 1, together with their wighted average.

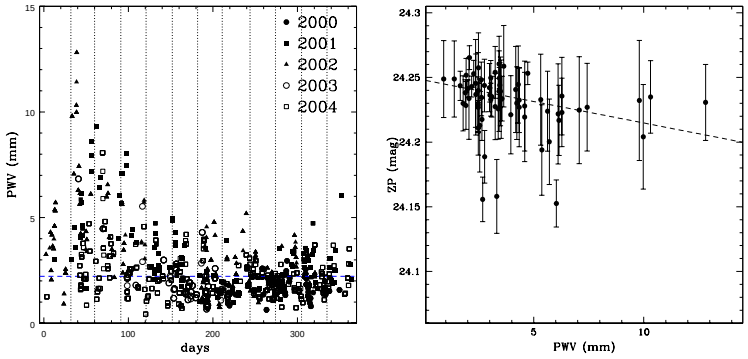

Fig. 2. Left: seasonal variation of the PWV (different symbols refer to different years). Right: an example of the dependency of the zero points on the PWV value.

Table 1. Extinction coefficient for each broad band filter J Js H and Ks and for each subsample or period (raw 1 to 9). The last raw (10) reports their average.

subsample	K_J	K_{Js}	K_H	K_{Ks}
P1	0.06±0.07	0.04±0.03	0.07±0.03	0.05±0.03
P2	0.04±0.04	0.00±0.04	0.02±0.03	0.02±0.01
P3	0.17±0.19	0.03±0.49	0.16±0.10	0.09±0.05
P4	0.10±0.04	0.06±0.01	0.03±0.01	0.02±0.09
P5	0.08±0.03	0.05±0.03	0.03±0.02	0.05±0.01
P6	–	–	–	–
P7	0.04±0.06	0.02±0.03	0.03±0.02	0.07±0.01
P8	0.15±0.06	0.03±0.03	0.04±0.03	0.06±0.01
P9	0.09±0.01	0.06±0.01	0.04±0.01	0.06±0.01
all	0.09±0.01	0.05±0.01	0.04±0.01	0.06±0.01

3 Determining the color terms

The LCO and ISAAC filter transmission curves are -supposedly- very similar. However, this was never verified observationally. Therefore, on July 19th 2005 we used technical time to observe 8 red Persson standard stars. The color terms or color corrections, χ, is the slope in the linear fit of the difference $(m_{\mathtt{LCO}} - m_{\mathtt{ISAAC}})$ versus the color $(\mathrm{J\text{-}Ks})_{\mathtt{LCO}}$ ($m_{\mathtt{LCO}} - m_{\mathtt{ISAAC}}$ being alternatively $\mathrm{J}_{\mathtt{LCO}}$-$\mathrm{J}_{\mathtt{ISAAC}}$, $\mathrm{J}_{\mathtt{LCO}}$-$\mathrm{Js}_{\mathtt{ISAAC}}$, $\mathrm{H}_{\mathtt{LCO}}$-$\mathrm{H}_{\mathtt{ISAAC}}$ and $\mathrm{Ks}_{\mathtt{LCO}}$-$\mathrm{Ks}_{\mathtt{ISAAC}}$) . The results are tabulated in Table 2 together with the standard star names, colors and instrumental magnitude differences in each band.

References

1. A. Manduca & R.A. Bell: PASP **91**, 848 (1979)

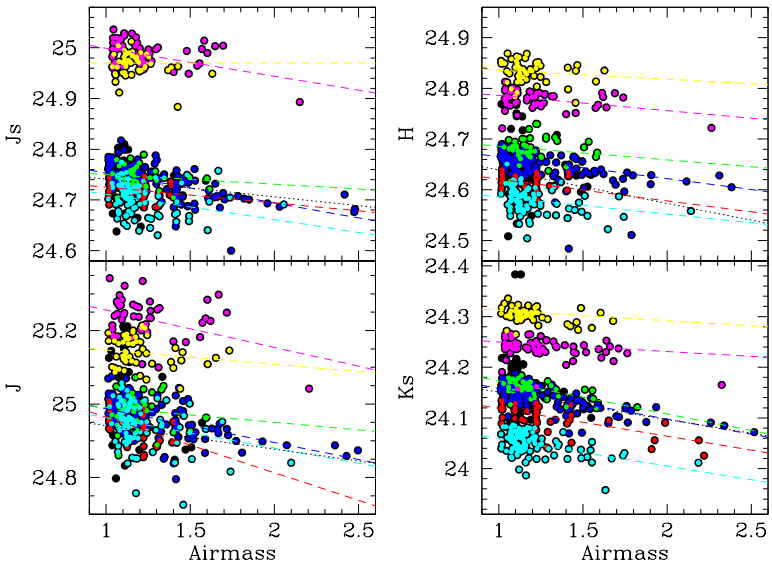

Fig. 3. Cleaned ZP vs airmass and Bouguer curve for each period and each filter.

Table 2. Color terms and the standard star used to compute those.

star	J-Ks	J-J_{ISAAC}	J-Js_{ISAAC}	H-H_{ISAAC}	K-Ks_{ISAAC}
cskd-21	0.724	0.31±0.03	0.03±0.03	-0.20±0.03	-0.67±0.04
cskf-12	1.110	0.32±0.02	0.03±0.02	-0.19±0.02	-0.69±0.02
cskf-14s	1.734	0.36±0.03	0.02±0.03	-0.29±0.02	-0.67±0.03
cskd-20	1.826	0.33±0.03	-0.01±0.03	-0.21±0.02	-0.69±0.03
cskd-9	2.219	0.29±0.05	-0.03±0.04	-0.18±0.04	-0.65±0.04
cske-23	2.735	0.35±0.04	-0.01±0.03	-0.24±0.02	-0.69±0.03
cskd-34	2.826	0.29±0.03	-0.04±0.03	-0.20±0.03	-0.68±0.03
cskd-16	2.863	0.32±0.03	-0.03±0.03	-0.19±0.03	-0.67±0.03
	χ	-0.00±0.01	-0.03±0.01	0.00±0.01	-0.00±0.01

2. S.E. Persson, D.C. Murphy, W. Krezeminsky et al: AJ **116**, 2475 (1998)